Available online at www.sciencedirect.com
SCIENCE DIRECT®
Sensors and Actuators B 109 (2005) 159–166
SENSORS AND ACTUATORS B CHEMICAL
www.elsevier.com/locate/snb

Assemblies of $TPPS_4$ porphyrin investigated by TEM, SPM and UV–vis spectroscopy

Valentinas Snitka [a,*], Mindaugas Rackaitis [b], Raminta Rodaite [a]

[a] *RC for Microsystems and Nanotechnology, Kaunas University of Technology, Kaunas LT 51369, Lithuania*
[b] *Bridgestone/Firestone Research, LLC, Akron, OH 44317-000, USA*

Available online 18 April 2005

Abstract

The aggregates of the tetrakis(4-sulfonatophenyl)porphyrin ($TPPS_4$) growth from solution on flat solid crystalline hydrophilic (mica, glass, Si) and hydrophobic (graphite) substrates were investigated. The spatial structure of $TPPS_4$ deposited on the surface was imaged using transmission electron microscopy (TEM), scanning atomic force microscopy (AFM). Scanning tunneling microscopy (STM) visualized porphyrin rings structure with molecular resolution. The aggregation of $TPPS_4$ was investigated by UV–vis spectroscopy. The investigation revealed a three-dimensional rod and wheel-like molecular order of the $TPPS_4$ porphyrin assemblies, while a corresponding shorter and monodisperse oligomer exhibited 2D ribbon-like structure. The $TPPS_4$ porphyrin molecules self-assemble into micrometer-long nanorods and fibers on substrate surface. Their cross-section was determined quantitatively by scanning force microscopy; this revealed a typical thickness of two or four molecular layers and a width of tenths of molecule diameter. This indicates that the molecules are fully extended in the ribbons oriented with the conjugated backbone with the 54.7° to the long axis of the rod. We propose here $TPPS_4$ ribbons as polymolecular architectures, which are building blocks of $TPPS_4$ rods and built from the homoassociated porphyrin molecules. The $TPPS_4$ nanoribbons could be used in a molecular-scale electronic device.

Keywords: Nanostructures; Porphyrin; Scanning probe microscopy; Self-assembly

1. Introduction

Organized self-assembly of molecules and self-organization is the central issue to the utilization of nanoscaled materials in the "bottom-up" approach of nanotechnology for future manufacturing [1]. Self-assembled, self-organized and covalent porphyrin arrays provide a versatile tool and are of fundamental importance as attractive building blocks for the modular construction of tailored field-responsive materials and potential applications in the design of sensors, catalysts, electronic and photonic devices, molecular sieves and solar energy conversion [2–6]. The design and construction of novel porphyrin architectures with well-defined geometries is an area of increasing current interest [7–8]. This requires an accurate control of the molecular arrangements over a wide range of length-scales, spanning from micrometers down to the molecular size. No covalent intermolecular forces have been used to engineer highly ordered three-dimensional (macro) molecular architectures where the single building blocks are held together by specific interactions, such as metal–ligand bonding, hydrogen bonding or π–π stacking. On the other hand, the self-assembly at the solid–liquid interface has been successfully used to control the molecular arrangement in two dimensions [9].

Four steps [10] can describe the organization and structure of matter into functional nanoscaled materials. The primary structure is molecular structure, well-understood and controlled by principles of organic chemistry. The secondary structure is a supramolecular structure, well-developed field based on known principles. The tertiary structure describes how the super molecules interact to form a higher order matter. The area made a significant progress to predict and design hierarchical structure, but is still developing. The last, the quaternary structure, describes how the self-assembled or self-organized material self-incorporates into the devices and

* Corresponding author. Tel.: +370 37 451588; fax: +370 37 451588.
E-mail address: vsnitka@ktu.lt (V. Snitka).

0925-4005/$ – see front matter © 2005 Elsevier B.V. All rights reserved.
doi:10.1016/j.snb.2005.03.027

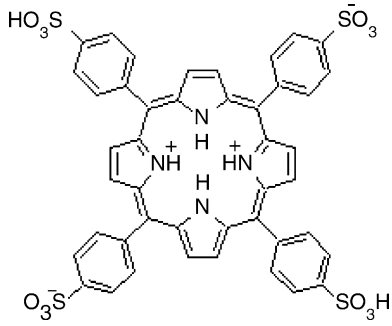

Fig. 1. Structure of the $TPPS_4$ porphyrin diacid ($H_4TPPS_4^{2-}$) in pH 1 solution.

builds interconnections to the macroscopic world. This field is at the starting point of its development. The intense research was made to understand the phenomena of porphyrin and related compounds aggregation [11–16]. The driving force for self-association in aqueous solution for such a class of molecules is the enthalpically driven attractive interaction between the π-systems, leading to the formation of stacks of molecules [13]. One of the well-known molecular assemblies of this kind is *J*-aggregates [12]. The aggregates are characterized through a new and sharp optical absorption band (*J*-band), which is shifted to larger wavelengths with respect to the long wavelength absorption band of the monomers at about 400 nm (the Soret band), followed by several weaker absorptions (*Q*-bands) at higher wavelengths (from 450 to 700 nm). According to several models [14–20], the aggregates should rather form two-dimensional systems of chromophores. The structure of the $TPPS_4$ porphyrin molecule in acid aqueous solution is shown in Fig. 1 [14].

These one- or two-dimensional models have further been modified to account for the optical activity of *J*-aggregates, observed in the presence of chiral auxiliaries [21,22]. The structure of $TPPS_4$ *J*-aggregate is presented in Fig. 2 and porphyrin molecules make an angle with the stacking direction [17]. It is common to all models that they explain specific experiments very well. However, their weak point is that they are often insufficiently founded by structural data.

On the other hand, the supramolecular structure of *J*-aggregates, i.e., their aggregation number, geometrical size and morphology, is not fully understood yet and controversially discussed. In particular, by use of no intrusive experimental techniques it became apparent that the spectroscopically determined aggregation numbers do not correspond to the geometrical size of the aggregates [23,24]. This conclusion is supported by results of picoseconds spectroscopy, suggesting large aggregates composed of many thousands of dye monomers [25].

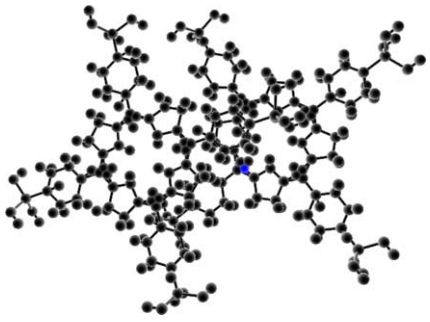

Fig. 2. Fragment of the structure of $TPPS_4$ *J*-aggregate.

To obtain detailed structural information about the supramolecular organization on surface for porphyrin self-assembled arrays the scanning tunneling microscopy (STM) [9,26–29], atomic force microscopy (AFM) [16,28,29] and scanning near field optical microscopy (SNOM) [30,31] were employed in the last years. Scanning probe microscopy plays a paramount role, since they allow one to explore organic surfaces on different scale lengths in various ambients [32].

In this paper, we report on the first study of molecularly resolved images of $TPPS_4$ porphyrin self-assembly at the solid–liquid interface and on the growth of this macromolecule into molecularly defined ribbons on graphite. Herein we report the results on the homoassociation of the meso-tetra(4-sulfonatophenyl)porphine (TPPS) in acidic media and self-assembly on the surface in order to infer about the building architecture from revealed cooperative effects of the self-assembly of porphyrin structures and application of scanning probe microscopies to investigate self-assembled architectures of porphyrin aggregates from the micron-scale to molecular-level on flat solid substrates.

The aim of this study was to correlate the spectroscopic pattern with the aggregate's molecular and supramolecular structure and to confirm experimentally the aggregation model suggested by authors in the early work [29].

An understanding of these effects is essential to obtain the self-organizing condensed phases of porphyrins with tailored properties for various applications.

2. Experimental

2.1. Materials

The tetra sodium salt of tetrakis-5,10,15,20(4-sulfonatophenyl) porphine was obtained from Porphyrin Products (Logan, UT) and was used without further purification. The *J*-aggregate solutions were prepared by dissolving $TPPS_4$ in acidic aqueous medium (HCl was added to reach pH 1) at the concentration range 1×10^{-4} to 2×10^{-6} M. To stabilize the aggregates formation the solution was left at room temperature for aggregation for 10 days, before the thin films preparation. The *J*-aggregates of $TPPS_4$ formed after solution preparation was confirmed by absorption spectra.

2.2. Preparation of porphyrin films

Highly oriented pyrolytic graphite (HOPG), glass, mica and silicon were chosen as supporting substrates. The thin films of $TPPS_4$ were prepared by drop casting solutions and

allowing the solvent to evaporate at room temperature in the dust-free environment, dipping substrate into solution or spin-coating technique at 100 rpm. Then the sample was dried in ambient air. The $TPPS_4$ thin films were generally deposited from 1×10^{-4} and 1×10^{-5} M solution.

2.3. Scanning force and tunneling microscopy

Muscovite mica slices for atomic force microscopy measurements were cut into discs with a punch and die set in order to produce readily cleavable edges. The glass covers for microscopy were used as glass substrates without any additional washing procedure. Hydrophilic silicon substrates were prepared by washing plates, cut from standard Si wafers, in a solution of 4.6% HCl and 3.5% H_2O_2 in MilliQ-grade water at 85° C for 5 min under the ultrasonic treatment.

The scanning tunneling microscopy measurements were made on HOPG samples. Molecular resolution was achieved and by varying the tunneling parameters, it was possible to visualize the HOPG lattice underneath and therefore to calibrate the piezo in situ. Droplet of sample solution was placed onto freshly cleaved highly oriented pyrolithic graphite and was allowed to dry at ambient conditions for 1 h. The sample was promptly imaged after with STM. The size of the homogeneous film sections depends on details of the preparation, including the solvent; this will be discussed elsewhere. High-resolution atomic force microscope measurements were made with a home-built AFM interfaced with NT-MDT control electronics (NT-MDT Inc., Zelenograd, Moscow, Russia) and AFM and STM measurements with a Nanoscope III Multi-mode (Veeco Metrology, Sunnyvale, CA).

The dry samples were investigated by SFM in the contact and tapping mode in a range of scan lengths from 5 to 0.1 μm, and using commercial Si cantilevers NSG11 series (length 100 μm and width 35 μm) with a force constant 11 Nm^{-1} and tip curvature 10 nm and resonance frequency 255 kHz (NT-MDT). The Pt/Ir commercial tunneling tips were used for STM measurements. The ribbon widths were measured [25] from images with a resolution of 512 pixels × 512 pixels and scan lengths 20 nm to 3 μm, while their heights were determined by the use of the facilities of the SPIP (Image Metrology) and NT-MDT softwares. Several tens of images were processed for each polymer length in order to minimize the influence of the choice of sample area and to reduce the statistical error.

2.4. Transmission electron microscopy (TEM)

TEM images were obtained with Hitachi S-4800 electron microscope in STEM mode. Acceleration voltage was 30 kV and emission current was 10 μA. Working distance was equal to 8 mm. Droplet of sample solution was placed onto the 200 mesh TEM grid with carbon film coating and was allowed to dry at ambient conditions. After that sample was either directly imaged or additionally stained with RuO_4 vapor. Staining was performed in covered petri dish where specimen containing grids were placed in the center of the dish and droplets of 0.5% aqueous solution of RuO_4 (EMS sciences) were placed around the grid. After 10 min, grids were removed and used for imaging.

2.5. Spectroscopy

Solution and monolayer spectra for the UV–vis experiments were obtained on an Ocean Optics diode array spectrophotometer to confirm the *J*-aggregates formation. A series of different solution concentrations of $TPPS_4$ were prepared and their absorbance at the Soret band maximum (~432 nm) was used to calculate the solution extinction coefficients using the Beer–Lambert law [22]. To obtain the monolayer absorption spectra, each glass cover slip was scanned before and after self-assembly of porphyrin film and the difference between the two spectra was the porphyrin monolayer absorption spectrum.

3. Results and discussion

3.1. Aggregation of $TPPS_4^{2-}$

The measured UV–vis spectrum of the acid solutions (see Fig. 3) has absorption maxima at 423, 490 and 705 nm, which has to be attributed to the formation of *J*-aggregates (490 nm), which at higher concentrations give H-aggregates (420 nm) [8]. In the dry films, an increased absorption appears in the region about 450 nm. This suggests that the simple dipole exciton coupling model, which explains the absorption spectra of the homoassociate solutions through two independent one-dimensional couplings (H- and *J*-aggregation), cannot be applied to the condensed phase and the collective 2D or 3D exiton model should be applied [33].

3.2. Transmission electron microscopy

In the evaporation of a drop of the solution, the TPPS film develops from the border to the center of the drop. The film

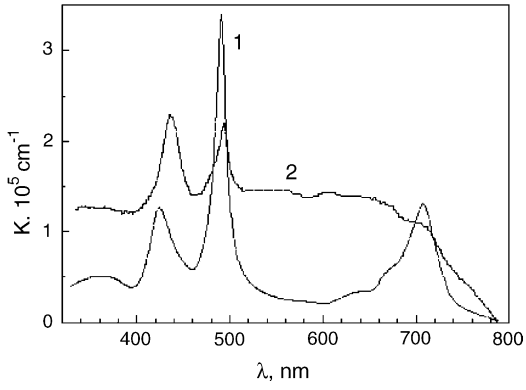

Fig. 3. UV–vis absorption spectra of $TPPS_4$ solution; (1) concentration 1×10^{-4} M, (2) 1×10^{-5} M.

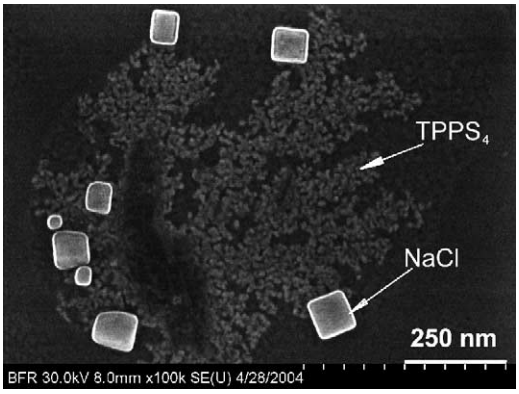

Fig. 4. SEM microphotograph of $TPPS_4$ aggregates and NaCl crystals obtained on carbon film after evaporation of solution.

surface retains water as it is seen from the force–displacement curves of AFM measurements. The water content depends on the water–vapor pressure of the surrounding atmosphere. The films show an organic phase, which incorporates NaCl crystals (see Fig. 4). These NaCl crystals rise at the periphery of surface of the organic phase or appear as a single crystal up to 0.5 μm in diameter. The $TPPS_4$ phase is textured in the form of elongated fiber-like or a wheel-like structures (Fig. 5).

The detail analysis of TEM images reveled that the wheel structures are the self-assembly of ring-type tetrameric structures with typical diameter of ∼10 nm. The ring-type structures consist of four segments with diameter of ∼4 nm. It is in good agreement with the dimensions of porphyrin ring (1.96 nm) and dimmer (3.16 nm) [34]. The diameter of the wheel structures varies from about 10 nm up to 250 nm. The central parts of the wheel is composed of phorphyrin dimmers and have a planar structure, in contrast with peripheral area of the wheel composed in 3D structure from TPPS dimmers aggregates of tetrameric structure. The cross-section of strip-like structure revealed by TEM have a 8–9 nm in diameter as it was obtained from images using the SPIP software and pixels count (Fig. 6).

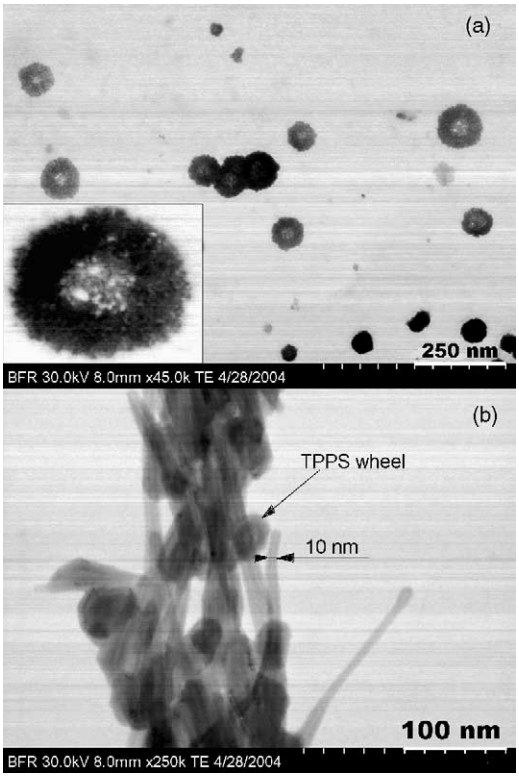

Fig. 5. TEM images: (a) wheel-like structures; (b) aggregate of stripe-like and wheels structures.

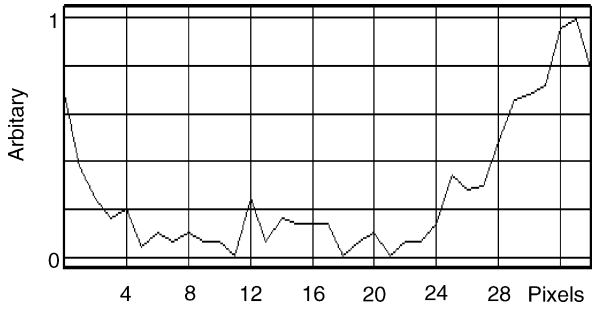

Fig. 6. Cross-section of strip-like $TPPS_4$ aggregate in Fig. 5b. Scale: 5 pixels = 2.5 nm.

3.3. Atomic force microscopy

AFM was used to perform quantitative measurements of molecular arrangements in the wide range of imaging-scales (100 nm to 5 μm) and are presented in Fig. 7. The fracture of the film observed by AFM shows that the fiber-like structures are stacked in a ribbon Fig. 7(b) of different structure, depending on the spot location on the $TPPS_4$ drop area. The ribbons consist of nanorods with width of 18–20 nm and height 8–10 nm. The nanorods are built of bricks of parallelogram form with the dimensions ∼34 nm × 56 nm and conclusion can be made from experiment that it consist of the two smaller parts. The angle between the short axis of building bricks of ribbons and ribbon axis (see Fig. 7c) measured by means of SPIP software was in the range of 51–56° which corresponds with the results on ZnP_3 porphyrin aggregation of the work [34]. The cross-section of double-rod ribbon, presented in Fig. 8, clearly demonstrates the double-rod structure of ribbon. The detail analysis of many images made at different scales demonstrate that the self-assembly of building blocks starts about some kind of backbone structure (see Fig. 7b). These backbone nanorods-type structures have a width of 18 nm and the height of 2–2.5 nm. The typical width of nanoribbons is 48–56 nm, but it was found the ribbons with the width around 100 nm. The dispersion of nanoribbon width can be a result of different orientation of the rods on the surface, different angle to the scanning direction. It was found that the parallelogram bricks represent a projection of wheel-like structures. These wheels-like assemblies are the building bricks of nanorods. It is seen at the end of nanorod in the Fig. 7c (marked by A). At the

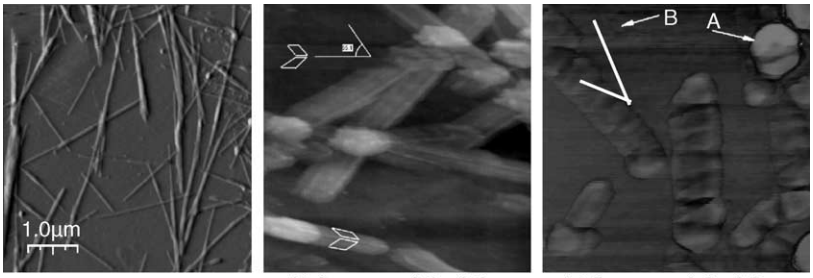

Fig. 7. AFM image of $H_4TPPS_4^{2-}$ morphologies on glass substrate.

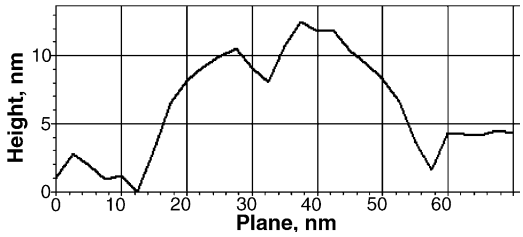

Fig. 8. Cross-section of double-rod ribbon.

same time, it was found that the wheel-type assemblies lay on the surface of substrate in the areas of nanorods and ribbons formation. Further investigation by AFM revealed that wheel structure consists of thin central part and four peripheral blocks (Fig. 9). The small structures are seen between the wheels. The dimensions of structures are 8–18 nm and height 0.8–1 nm. The cross-section of the wheel structure measured by AFM is presented on Fig. 10. The measured wheel height is 8 nm and diameter 80 nm. The next typical size of wheels observed—diameter 28 nm and height 2 nm. AFM investigations revealed the smallest building blocks with dimensions 12 nm × 28 nm × 2 nm, the next revealed structure have dimensions 20 nm × 56 nm.

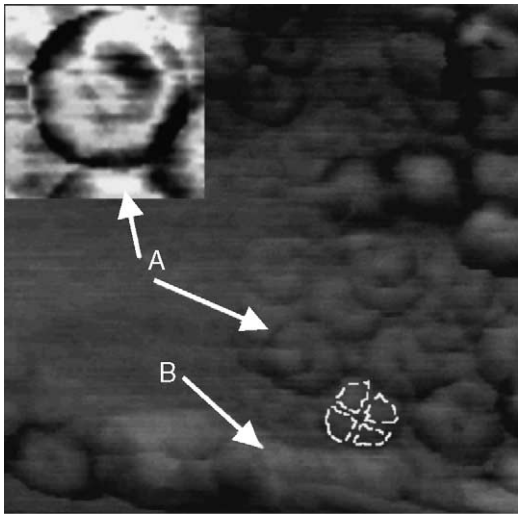

Fig. 9. The wheel-like structures (A) on the surface and the nanorod (B) assembled from the wheels. Scale: 500 nm × 500 nm.

3.4. Scanning tunneling microscopy

Fig. 11 shows STM images of $TPPS_4$ ribbon-like aggregates on HOPG surface prepared by drop evaporation. Fig. 11a is a STM topography scan intended to reveal the gross surface morphology of the aggregated structures. Within the 100 nm × 100 nm area it is clear seen a ribbon-like structure, which consist of thin rod-like structures, oriented along the long axis of the ribbon. The thin rod-like structures dimensions have a measured by the tools of SPIP software width ∼1.4–1.8 nm, which correspond to the diameter of $TPPS_4$ porphyrin molecule [35]. In the area marked (A), it is seen a ring-like structures. The wide of perpendicular to the ribbon axis formations have an average width of $\Delta L = 8$ nm. It correlates very well with the results of AFM and TEM investigations. The image demonstrates the fact that the self-assembly of $TPPS_4$ from the acid aqueous solution during the evaporation into solid-state film is going on the sample surface. The dispersion of monomer and dimmer size aggregates on the surface and the step-by-step evolving process to the ribbon-like structure was imaged on the surface.

The higher resolution STM scan shown in Fig. 11b indicates the formation of ordered molecular arrays along the ribbon axis. The bright dots in Fig. 11b (marked A) forming the periodical linear array have a diameter of 0.7 nm and are ascribed to the $TPPS_4$ molecules phenyl ring. The measured distance was 1.8 nm between the centers of the neighboring linear arrays. It fits very well into the dimensions range obtained by other works on porphyrin homoassociation [36]. This confirms the *J*-aggregation model of linear

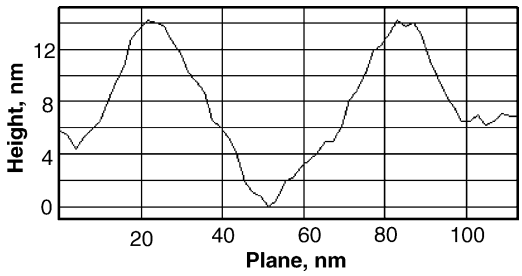

Fig. 10. The cross-section of wheel structure.

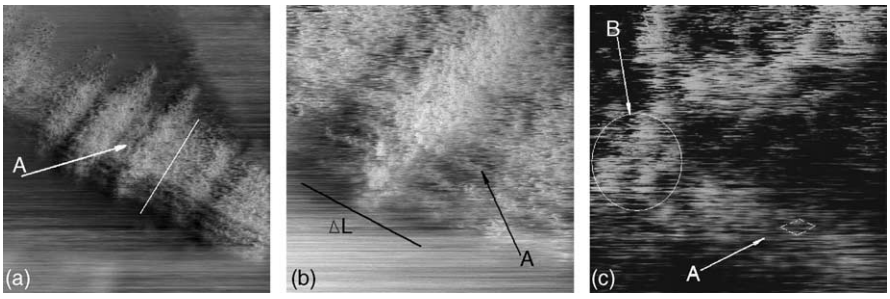

Fig. 11. Large-scale (100 nm × 100 nm) (a), middle-scale (20 nm × 20 nm) (b) and molecular-scale (5 nm × 5 nm) (c) STM images of the $TPPS_4$ assemblies on the HOPG surface. The tip potential and the tunneling current were, respectively, 1 V and 1.5 nA.

porphyrin molecules arrangement proposed in early works [20]. The atomic resolution STM scan shown in Fig. 11c indicates the graphite atomic structure (marked A) and a porphyrin molecule is seen as a propeller-like shape (marked B). The measured diameter of the molecule from the image cross-section was found 1.6 nm × 1 nm and the height 0.6 nm, which is in good agreement with other works on porphyrin molecules investigation [18,29]. As it is seen on the Fig. 11c, the molecule is connected to the nanowheel structure composed of a few molecules. The diameter of this formation was found ∼4 nm and the bright spot in the center of nanowheel is ascribed to the $TPPS_4$ molecule. The STM imaging results allow to make a statement that $TPPS_4$ porphyrin molecules self-assemble on the surface into nanoribbon-like structures by rod-like association of porphyrin molecules into linear structures and these linear structures grow in parallel to form a ribbon. The structures growth is based on the association of single molecules or complexes of several molecules to the association centers on the surface of the sample. The complexes tend to form a wheel-like structure ranging in diameter from several nanometers up to hundred of nanometers.

The self-assembled structures start as a 2D molecular pattern and molecules lie flat on the (0 0 1) plane of the HOPG. The conjugated backbones of porphyrin phenyl rings appear brighter than the sulfonic chains because of a stronger current. The spacing between neighboring parallel backbones along the long axis of ribbon, which can be attributed to the width of the molecules, amounts to ΔL=1.8 nm. It is close to the 1.9 nm calculated for the case with the sulfonic chains extended. This indicates that the side-chains are well oriented between adjacent parallel backbones. From the comparison of the porphyrin molecules data value with the spacing between neighboring backbones evaluated from molecularly resolved STM images, we suggest that the $TPPS_4$ ribbons grow are not equally distributed of one or few monolayers thick. The connecting structures have one monolayers height and one molecule width and building blocks have a height up to 10 monolayers with their sulfonic chains oriented perpendicular to the substrate (Fig. 11). The width and the height of the well-developed ribbons are constant for some straight ribbon sections; however, they are not constant for with single, triple and even higher multilayers, however, they are not constant for the whole sample. The apparent widths shift to higher values with increasing length of the pseudopolymer (Fig. 7). Since the absolute value of the width is of the order of the length of a single molecule, it is concluded that the extended molecules are packed parallel to each other with their long molecular axis perpendicular to the long ribbon axis, as represented in the proposed ribbon model (Fig. 12).

The width of the ribbon is attributed to the molecular weight of molecules, which implies that molecules with similar molecular weights phase-segregate into ribbon sections with homogeneous widths. This segregation phenomenon governs the formation of the ribbons, requires a small degree of polymerization, and is likely to be favored by a low macromolecular polydispersity. The ribbons structures self-organize into long parallel rods in the central part of the drop with growing concentration of $TPPS_4$ molecules during evaporation (Fig. 13). The structure of rods has two conjugated ribbon lines and the width of the rod is 40 nm and the height 1.5 nm. The dimensions of the building blocks (ribbons) are 20 nm × 40 nm.

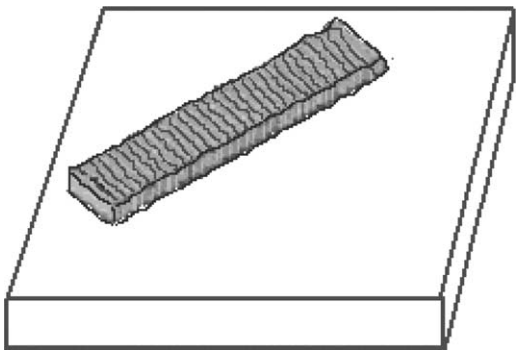

Fig. 12. Schematic representation of molecular ribbons of $TPPS_4$ adsorbed on the HOPG surface. (a) Ribbons are made of several nanorods packed parallel one to each other. (b) Each nanorod is typically made of ten $TPPS_4$ molecules packed, with the sulfonic chains parallel to the basal plane of the substrate.

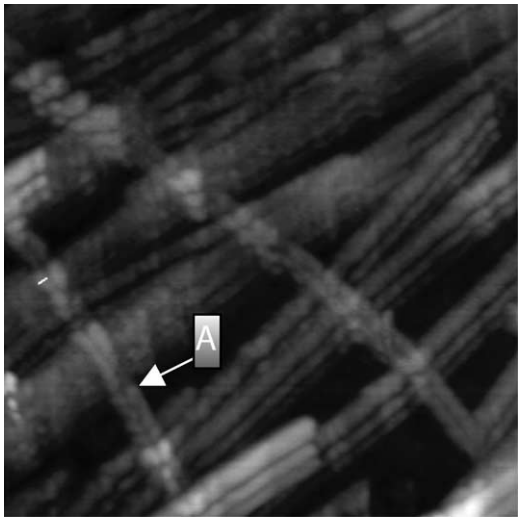

Fig. 13. The double-line structure of $TPPS_4$ porphyrin is self-organized from the building blocks (ribbons). Scan area: 500 nm × 500 nm. The dimensions of building block (A) are 20 nm × 40 nm.

4. Conclusions

We have characterized the self-assembly of a tetrakis(4-sulfonatophenyl)porphyrin on flat solid crystalline hydrophilic (mica, glass, Si) and hydrophobic (graphite) substrates. It is a first time demonstration of molecularly resolved images of $TPPS_4$ aggregates formation. At the interface between graphite, glass, Si and an acidic aqueous solution molecularly ordered structures are formed. The different morphologies were observed, as depicted in Figs. 7, 9 and 11. The wheel-like and rod-type formations were found. The self-organization and grow of long $TPPS_4$ rods is based on the self-assembly of building blocks (nanoribbons) with typical dimensions of 20 nm × 40 nm, but it is common 80–100 nm width cross-section. The rods have a double-line structure; can be organized in two layers with flat teramer in cross-section. The building blocks (ribbons) are made of several nanorods packed parallel one to each other. Each rod has a typical width 8–9 nm, which corresponds with five molecules or three dimmers dimension. The height of ribbon varies from the monolayer to several layers. The nanorods in ribbon are connected by monomolecular chains. The wheel-like structures found by TEM, AFM and STM as possible building blocks for another type of rods (Fig. 9) vary in dimensions from few nanometres to hundred of nanometres.

Porphyrin-based materials herein studied showed nanoporous surfaces, and their potential applications are promising. In fact, nanoporousity and controlled orientation usually translate into high efficiency for sensing devices due to the high surface area. Moreover, the superficial feature may be chemically tailored by using different metals or spacers, making it suitable for sensors.

Acknowledgment

This work supported by Lithuanian State Science and Study Fund under the project “FunNano”.

References

[1] Implications of Emerging Micro- and Nanotechnologies, The National Academy Press, Washington, D.C., National Research Council, 2002. p. 231.
[2] P. Hambright, in: K. Kadish, K.M. Smith, R. Guilard (Eds.), The Porphyrin Handbook, vol. 3, Academic Press, New York, 2000, pp. 129–210.
[3] M.A. Awawdeh, J.A. Legaco, H.J. Harmon, Solid-state optical detection of amino acids, Sens. Actuators B 91 (2003) 227–230.
[4] A.A. Umar, M.M. Salleh, M. Yahaya, Self-assembled monolayer of copper(II) meso-tetra(4-sulfanatophenyl) porphyrin as an optical gas sensor, Sens. Actuators B 101 (2004) 231–235.
[5] N.A. Rakow, K.S. Suslik, A colorimetric sensor array for odour visualisation, Nature 406 (2000) 710–712.
[6] D. Delmare, R. Meallet, C. Bied-Charreton, R.B. Pansu, Heavy metal ions detection in solution, insol gel and with grafted porphyrin monolayers, J. Photochem. Photobiol. 124 (1999) 23–28.
[7] K.S. Suslik, N.A. Rakov, M.E. Kosak, J.H. Chou, The materials chemistry of porphyrins and metalloporphyrins, J. Porphyrins Phthalocyanines 4 (2000) 407–413.
[8] J.T. Hupp, S.T. Nguyen, Functional nanostructured molecular materials, Interface Fall (2001) 28–32.
[9] J.A.W. Elemans, M.C. Larsen, J.W. Gerritsen, H. Kempen, S. Speller, R.J.M. Nolte, A.E. Rowan, Scanning probe studies of porphyrin assemblies and their supramolecular manipulation at a solid–liquid interface, Adv. Mater. 15 (2003) 2070–2073.
[10] C.M. Drain, J.T. Hupp, K.S. Suslik, M.R. Wasielevski, X. Chen, A perspective on four new porphyrin-based functional materials and derivatives, J. Porphyrin Phthalocyanines 6 (2002) 243–258.
[11] H. Berlepsch, C. Bottcher, A. Ouart, C. Burger, S. Dahne, S. Kirstein, Supramolecular structures of J-aggregates of carbocyanine dyes in solution, J. Phys. Chem. B 104 (2000) 5255–5262.
[12] T. Kobayashi (Ed.), J-Aggregates, World Scientific Publishing, Singapore, 1996.
[13] J. Hofkens, L. Latterini, P. Vanoppen, H. Faes, K. Jeuris, S. DeFeyter, J. Kerimo, P.F. Barbara, F.C. DeSchryver, A.E. Rowan, R.J.M. Nolte, Mesostructure of evaporated porphyrin thin films: porphyrin wheel formation, J. Phys. Chem. B 101 (1997) 10588–10598.
[14] O. Ohno, Y. Kaizu, H. Kobayashi, J-aggregate formation of a water-soluble porphyrin in acid aqueous media, J. Chem. Phys. 99 (1993) 4128–4139.
[15] A. Pawlik, S. Kirstein, U. De Rossi, S. Dahne, Structural conditions for spontaneous generation of optical activity in J-aggregates, J Phys. Chem. B 101 (1997) 5646–5649.
[16] S. Okada, H. Segawa, Substituent-control exciton in J-aggregates of protonated water-insoluble porphyrins, J. Am. Chem. Soc. 125 (2003) 2792–2796.
[17] H. Kano, T. Saito, T. Kobayasashi, Dynamic intensity borrowing in porphyrin J-aggregates revealed by sub-5-fs spectroscopy, J. Phys. Chem. B 105 (2001) 413–419.
[18] K. Kano, K. Fukuda, H. Wakami, R. Nishiyabu, R.F. Pasternack, Factors influencing self-aggregation tendencies of cationic porphyrins in aqueous solution, J. Am. Chem. Soc. 122 (2000) 7494–7502.
[19] R.F. Pasternack, C. Fleming, S. Herring, P.J. Collings, J. dePaula, G. DeCastro, E.J. Gibbs, Aggregation kinetics of extended porphyrin and cyanine dye assemblies, Biophys. J. 79 (2000) 550–560.

[20] R. Rubires, J. Crusats, Z. El-Hahemi, T. Jaramillo, M. Lopez, E. Valls, J.A. Farrera, J.M. Ribo, Self-assembly in water of the sodium salts of meso-sulfonatophenyl substituted porphyrins, New J. Chem. (1999) 189–198.
[21] X. Huang, K. Nakanishi, N. Berova, Porphyrins and metalloporphyrins: versatile circular dichroic reporter groups for structural studies, Chirality 12 (2000) 237–255.
[22] H. Kano, T. Saito, T. Kobayasashi, Dynamic intensity borrowing in porphyrin J-aggregates revealed by sub-5-fs spectroscopy, J. Phys. Chem. B 105 (2001) 413–419.
[23] W.J. Harrison, D.L. Mateer, G.T. Tiddy, Liquid-crystalline J-aggregates formed by aqueous ionic cyanine dyes, J. Phys. Chem. 100 (1996) 2310–2314.
[24] H. Yao, H. Ikeda, N. Kitamura, Surface-induced J-aggregation of pseudoisocyanine dye at a glass/solution interface studied by total-internal-reflection fluorescence spectroscopy, J. Phys. Chem. B 102 (1998) 7691–7694.
[25] B. Herzog, K. Huber, H. Stegemeyer, Aggregation of a Pseudoisocyanine Chloride in Aqueous NaCl Solution, Langmuir 19 (2003) 5223–5232.
[26] P. Samori, A. Fechtenko, F. Jackel, T. Bohme, K. Mullen, J.P. Rabe, Supramolecular staircase via self-assembly of disk-like molecules at the solid–liquid interface, J. Am. Chem. Soc. 123 (2001) 11462–11467.
[27] L. Pirondini, A.G. Stendardo, S. Geremia, M. Campagnolo, P. Samori, J.P. Rabe, R. Fokkens, E. Dalcanale, Dynamic materials through metal-directed and solvent-driven self-assembly of cavitands, Angew. Chem. Int. Ed. 42 (2003) 1384–1387.
[28] T. Milic, J.C. Garno, J.D. Batteas, Self-organization of self-assembled tetrameric porphyrin arrays on surfaces, Langmuir 20 (2004) 3974–3983.
[29] R. Rotomskis, R. Augulis, V. Snitka, R. Valiokas, B. Liedberg, Hierarchical structure of $TPPS_4$ J-aggregates on substrate revealed by atomic force microscopy, J. Phys. Chem. B 108 (9) (2004) 2833–2838.
[30] A. Miura, Y. Yanagawa, N. Tamai, Mesoscopic structures and dynamics of merocyanine J-aggregate studied by time-resolved fluorescence SNOM, J. Microsc. 202 (2001) 425–429.
[31] A.K. Miura, K.S.X. Matsumura, N. Tamai, Time-resolved and near-field scanning optical microscopy study on porphyrin J-aggregate, Acta Phys. Pol. 94 (1998) 835–846.
[32] J.K. Gimzewski, C. Joachim, Nanoscale science of single molecules using local probes, Science 283 (1999) 1683–1688.
[33] J.M. Ribo, R. Rubires, Z. El-Hachemi, J.A. Farrera, L. Campos, G.L. Pakhomov, M. Vendrell, Self-assembly to ordered films of the homoassociate solutions of the tetrasodium salt of 5,10,15,20-tetrakis 4-sulfonatophenyl porphyrin dihydrochloride, Mater. Sci. Eng. C 11 (2000) 107–115.
[34] A.L. Bramblett, M.S. Boeckl, K.D. Hauch, B.D. Ratner, T. Sasaki, J.W. Rogers, Determination of surface coverage for tetraphenylporphyrin monolayers using ultraviolet visible absorption and X-ray photoelectron spectroscopies, Surf. Interface Anal. 33 (2002) 506–515.
[35] P. Terech, C. Scherer, B. Deme, R. Ramasseul, Aggregation of a Zn(II) complex of a long-chain triester of meso-tetrakis [*p*-carboxylphenyl] porphyrin in hydrocarbons: structure of tetrameric rod-like assemblies, Langmuir 19 (2003) 10641–10647.
[36] A.D. Schwab, D.E. Smith, C.S. Rich, E.R. Young, W.F. Smith, J.C. de Paula, Porphyrin nanorods, J. Phys. Chem. B 107 (2003) 11339–11345.

Biographies

Valentinas Snitka received his PhD from Kaunas University of Technology, Lithuania, in 1976 and DrSc from Moscow Institute of Electronics Technology, in 1990. He is a director of Research Center for Microsystems and Nanotechnology at Kaunas University of Technology, Coordinator of Lithuanian Nanoscience and Nanotechnology Network. His current research is oriented to the molecular nanotechnology (synthesis of organic nanotubules, molecular wires), scanning probe microscopy instrumentation development and application for materials research, surface nanostructuring, sol–gel ferroelectric films for MEMS applications.

Mindaugas Rackaitis received a MS degree in applied physics in 1995 and a PhD in physics in 2000 from Kaunas University of Technology, Lithuania. From 2001 to 2004 he was a postdoctoral associate at The Pennsylvania State University. Currently he is a senior research scientist at Bridgestone Americas Center for Research and Technology. His research interests are in the field of material science and nanotechnology.

Raminta Rodaite obtained her Diploma in Engineering in Chemistry from Kaunas University of Technology in 2000. Currently she is a PhD student in Biophysics department, Kaunas Vytautas Magnus University, Lithuania.